

Nanoscale

Accepted Manuscript

This article can be cited before page numbers have been issued, to do this please use: S. Bera and S. Ghosh, *Nanoscale*, 2024, DOI: 10.1039/D4NR02494J.



This is an Accepted Manuscript, which has been through the Royal Society of Chemistry peer review process and has been accepted for publication.

Accepted Manuscripts are published online shortly after acceptance, before technical editing, formatting and proof reading. Using this free service, authors can make their results available to the community, in citable form, before we publish the edited article. We will replace this Accepted Manuscript with the edited and formatted Advance Article as soon as it is available.

You can find more information about Accepted Manuscripts in the [Information for Authors](#).

Please note that technical editing may introduce minor changes to the text and/or graphics, which may alter content. The journal's standard [Terms & Conditions](#) and the [Ethical guidelines](#) still apply. In no event shall the Royal Society of Chemistry be held responsible for any errors or omissions in this Accepted Manuscript or any consequences arising from the use of any information it contains.

ARTICLE

Alternating vs Random Amphiphilic Polydisulfides: Aggregation, Enzyme Activity Inhibition and Redox-responsive Guest Release

Sukanya Bera and Suhrit Ghosh*

Received 00th January 20xx,
Accepted 00th January 20xx

DOI: 10.1039/x0xx00000x

This paper reports synthesis an alternating copolymer (ACPs) with bio-reducible amphiphilic polydisulfide backbone and highlights the impact of the alternating monomer-connectivity on the self-assembly, morphology, chain-exchange dynamics, drug-release kinetics and enzyme-activity inhibition. Condensation polymerization between hydrophobic 1,10-bis(pyridin-2-ylidysulfaneyl)decane and hydrophilic 2,3-mercapto succinic acid (1.04:1.00 ratio) generates the amphiphilic ACP P1 ($M_w = 8450$ gm/mole, $\bar{D} = 1.3$), that exhibits self-assembly in water, leading to the formation of ultra-thin (height < 5.0 nm) entangled fibrillar network. In contrast a structurally similar amphiphilic random copolymer P2 shows truncated irregular disc-like morphology under the same condition. It is postulated that due to perfect alternating sequence of the hydrophobic and hydrophilic segments in P1, it's immiscibility-driven aggregation in water leads to a pleated structure, which further assembles to the observed long fibrillar structures, similar to crystallization-driven self-assembly. In fact, wide-angle X-ray diffraction analysis lyophilized P1 sample shows sharp peaks indicating its crystalline nature (% crystallinity $\sim 37\%$), which are completely missing for P2. Effect of such distinct self-assembly on the chain-exchange dynamics was probed by fluorescence resonance energy transfer (FRET) using 3,3'-dioctadecyloxycarbocyanine perchlorate (DiO) and 1,1'-dioctadecyl-3,3,3',3'-tetramethylindocarbocyanine perchlorate (DiI) as the FRET- donor and acceptor, respectively. DiI and DiO entrapped solutions of P1, when mixed, no prominent FRET appeared even after 24h. In sharp contrast, for P2, intense FRET emission noticed and the FRET ratio (~ 0.9) reached saturation in ~ 15 h, indicating much enhanced kinetic stability of P1 aggregates. Glutathione-induced release of encapsulated Nile red showed much slower kinetics for P1 compared to that of P2, corroborating with the observed slow chain-exchange dynamics of the highly stable alternating copolymer assembly. Further, the well-ordered assembly of P1 showed excellent surface functional group display (zeta potential -32 mV compared to -14 mV for P2) which resulted in effective recognition of α -chymotrypsin (Cht) protein surface by electrostatic interaction. Consequently, P1 could significantly ($> 70\%$) suppress the enzymatic activity of Cht, while in presence of P2, the enzyme was still active in $> 70\%$ efficacy.

Introduction

Amphiphilic polymers exhibit immiscibility driven aggregation in water leading to different nanostructures.¹ They are of interest in different applications including drug delivery, antibacterial materials, tissue engineering, protein delivery and others.² Most of such systems are block copolymers,¹⁻² other than relatively a smaller number of reports on amphiphilic homopolymers,³ random⁴ or alternating copolymers.⁵ Amongst them, alternating copolymers are unique in a sense that there is a defined sequence of the two different monomers⁶ in this structure. Owing to this unique sequence, alternating copolymers exhibit distinct self-

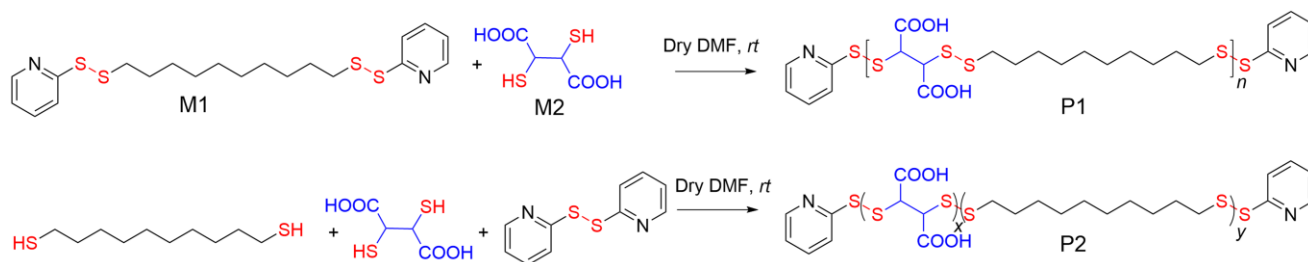
assembly behaviour⁷ or functional properties.⁸ Despite the first report on the synthesis of alternating copolymer of stilbene with maleic anhydride dates back to 1930,⁹ preparation of structurally diverse copolymers with alternating sequence remains to be a challenge through chain-growth mechanism. Increased difference in electron density, steric hindrance, pseudo connectivity or pre-defined sequence between the two comonomers are strategies, with limited success, for synthesis of alternating copolymers (ACPs) by chain polymerization.⁵ However, in step-growth polymerization between AA and BB type monomers, the resulting polymer intrinsically has the alternating sequence. Hence if these monomers can be designed in such a way that one is hydrophobic and the other is hydrophilic, it will produce amphiphilic ACPs without any ambiguity in their sequence. Similar strategies have been used for the synthesis of different amphiphilic ACPs which exhibit chain-folding regulated self-assembly or crystallization.¹⁰⁻¹¹ We envisaged such well-defined self-assembled systems may be highly relevant for biological applications, for which it is imperative to achieve

School of Applied and Interdisciplinary Sciences, Indian Association for the Cultivation of Science, 2A and 2B Raja S. C. Mullick Road, Kolkata, India-700032.
Email- psusg2@iacs.res.in

Supplementary Information available: [Synthesis of the polymers, materials and methods, additional self-assembly data and experimental detail]. See DOI: 10.1039/x0xx00000x

control over several important parameters such as functional group display, chain-exchange dynamics or stability.

protons. By comparing the intensity of the end group protons (He) and backbone proton (Ha), average degree of



Scheme 1: Synthesis of P1 and P2

In the recent past we have developed a synthetic methodology for making polydisulfides (PDSs) through condensation polymerization pathway.¹² In a sense it is a unique polymerization technique, in which any dithiol (AA) gets polymerized with commercially available 2,2'-Dipyridyl disulfide (BB) by thiol-disulfide exchange reaction. Although it is AA + BB type polymerization, at the end it produces the same polydisulfides, that would be achieved by oxidative polymerization of the dithiol monomer. We are particularly interested in disulfide containing polymers, as they present a bio-reducible linker,¹³ which can be degraded in presence of a glutathione, especially in the intracellular location due to its significantly higher concentration.¹⁴ We realized that this methodology can be easily extended to prepare amphiphilic ACPs with the degradable PDS backbone, which would enable testing the relevance of such perfectly sequenced polymers for aqueous self-assembly and biological applications. With this objective, in this manuscript we have synthesized an amphiphilic ACP with PDS backbone (P1, Scheme 1) and compared its self-assembly, chain-exchange dynamics, and enzyme activity inhibition with a structurally similar random copolymer (P2, Scheme 1).

polymerization could be calculated to be 17. UV/Vis spectrum showed (Fig. S1) a band ($\lambda = 250-300$ nm) corresponding to the end-groups, from which molecular weight of P1 was estimated to be 8560 gm/ mole, which showed a very good match with that estimated from size exclusion chromatography (SEC) (Fig S2) or end-group analysis using the NMR spectrum (Table 1).

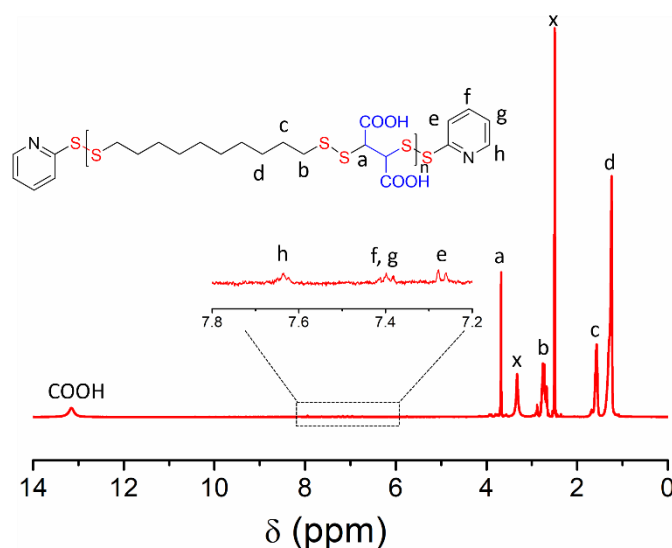


Fig. 1 ^1H NMR of P1 (solvent DMSO- d_6); Peaks marked with "X" come from the solvent.

Results and Discussion

Scheme 1 shows synthesis of P1 and P2. Monomer M1 was synthesized from commercially available 1,10-Decanedithiol by reacting it with excess 2,2'-Dipyridyl disulfide and isolated as pale-yellow oil in 58 % yield. Condensation polymerization reaction at rt between M1 (hydrophobic) and commercially available 2,3-dimercapto succinic acid (M2, hydrophilic) produced the desired poly(disulfide) based amphiphilic ACP P1. It was isolated as a colourless solid in 42 % yield. During the polymerization, intentionally M1 was taken in slight excess (M1: M2 = 1.04:1.00) for avoiding presence of reactive thiol groups at the chain-terminal. P1 was characterized by ^1H NMR (Fig 1) in which all the peaks could be assigned unambiguously. Enlarged view of selected region ($\delta = 7.0-8.0$ ppm) showed presence of characteristic peaks for the aromatic protons of the pyridyl-disulfide groups, present in the chain-ends. Also visible was the peak at $\delta = 13$ ppm for the carboxylic acid

Likewise, the amphiphilic random copolymer P2 was synthesized by condensation polymerization between 1,10-Decanedithiol, 2,3-dimercapto succinic acid (M2) and 2,2'-Dipyridyl disulfide, in which the reactive pyridyl-disulfide and the thiol groups were taken in 1.04: 1.00 ratio, while the two dithiols were taken in 1:1 ratio. It produced the amphiphilic random copolymer, which could be characterized by SEC studies (Fig. S2), ^1H NMR (Fig. S3) and UV/Vis (Fig. S1). Molecular weight of P2, estimated from SEC or end-group analysis was comparable to that of P1 (Table 1). From the end-group analysis by ^1H NMR, average number of hydrophobic and hydrophilic units are 9 and 10, respectively. It is imperative to note that the molecular weight and dispersity values for both polymers are almost identical, which makes

their comparison free of any intrinsic structural effects other than the monomer connectivity sequence. Also, the dispersity values in the range of ~ 1.2 for polymers synthesized by the step-growth route are appreciable and indicate well-defined polymerization.

Table 1: Molecular weight of P1 and P2. Theoretically estimated molecular weight value = 9870 gm.mol^{-1} using the stoichiometric imbalance and conversion 100 %.

Polymer	M_w (SEC) ^a gm.mol ⁻¹	Dispersity (Đ)	Mol. Wt. (NMR)	Mol. Wt. (UV)
P1	8500	1.25	6800	8600
P2	8700	1.21	7200	8300

^a SEC conditions: concentration = 5.0 mg/mL; solvent-DMF; standard-PMMA;

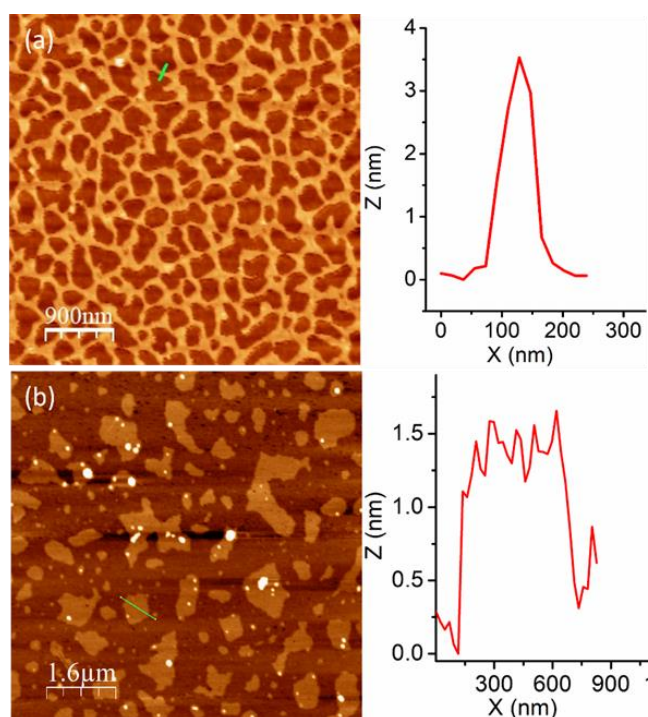


Fig. 2 AFM images of (a) P1 and (b) P2 aggregates. Height profile along the green line is shown in the right.

Aggregation of P1 was tested in aqueous medium in basic pH to ensure that the carboxylic acid groups remain as carboxylate. AFM image (Fig. 2a) shows long cylindrical structures with interconnected network formation.¹⁵ Interestingly height of these worm-like structure is $< 5.0 \text{ nm}$, indicating these are extremely thin flat structures. Contrary to P1, the random copolymer P2 shows irregular disc-like morphology (Fig. 2b) with height $< 2 \text{ nm}$, indicating significant difference in the aggregation behaviour of the alternating and random amphiphilic copolymers. It is proposed that, due to strictly alternating sequence of the hydrophilic and hydrophobic segments in P1, immiscibility driven aggregation in water leads to pleated structure (Fig. 3a), which further

assembles to the observed long fibrillar structures,¹⁵ similar to those observed for the crystallization-driven assembly.¹⁶ In fact, wide-angle X-ray diffraction analysis of the sample, obtained by lyophilization of the aqueous solution of P1, showed (Fig. 3b) sharp peaks at $2\theta = 12.8, 25.6, 32.2$ and 39.0° , indicating crystalline nature of the aggregate.¹⁷ In sharp contrast no such peaks were noticed for random copolymer P2 (Fig. 3b), which highlights the importance of the alternating sequence for the observed well-defined aggregation.

Container property of these polymer aggregates was examined by encapsulation of hydrophobic dye Nile red (NR). In both cases, NR-treated polymer solution showed intense red colour, indicating successful dye encapsulation in the hydrophobic pocket of these polymer aggregates. Fluorescence spectra showed typical emission band for NR. By concentration dependent fluorescence experiments (Fig. S4), critical aggregation concentration (CAC) of P1 and P2 were estimated to be roughly $15 \mu\text{g/mL}$ and $27 \mu\text{g/mL}$, respectively.

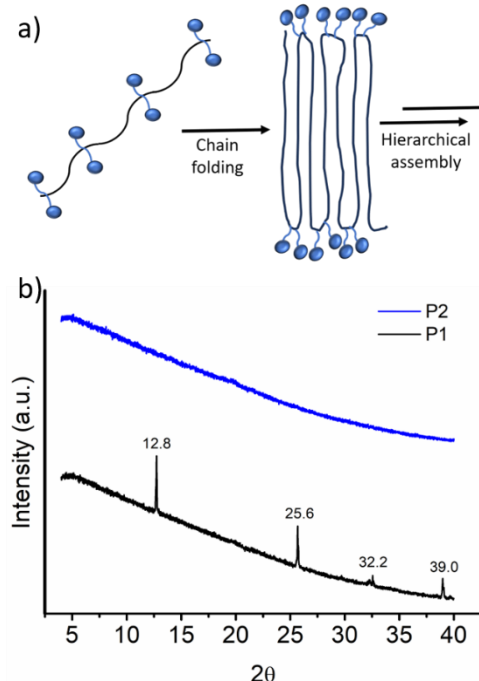


Fig. 3 (a) Schematic showing immiscibility driven assembly of P1 with crystalline nature; (b) Wide angle X-ray diffraction pattern of P1 and P2. Experiments were carried out with solid samples obtained after lyophilization of aqueous aggregates ($c = 3.0 \text{ mg/mL}$) of P1 and P2.

Next, we examined the chain-exchange dynamics of the aggregates of P1 and P2 by fluorescence resonance energy transfer (FRET) using 3,3'-dioctadecyloxycarbocyanine perchlorate (DiO) and 1,1'-dioctadecyl-3,3,3',3'-tetramethylindocarbocyanine perchlorate (Dil) as the FRET-donor and acceptor, respectively (Fig. S5).¹⁸ Dil and DiO were encapsulated separately in P1 aggregate and then the two different dye-encapsulated solutions were mixed together and the FRET-emission was monitored as a function of time (Fig. 4). Excitation was set at 485 nm corresponding to the absorption of the donor (DiO), which resulted in intense emission at 508

nm corresponding to DiO, but no such prominent emission band was noticed for the acceptor DiI at 570 nm, indicating negligible FRET. Emission spectra were recorded up to 24 h, when no increase in the FRET efficiency was noticed, rather it remained constant at a very low value of ~ 0.3 , which can also be due to the contribution from the direct excitation of the acceptor chromophore. This indicates a remarkable slow exchange dynamics in the P1 aggregate. In sharp contrast, for the P2 aggregate, after mixing DiO and DiI encapsulated solutions, FRET efficiency spontaneously reached to a very high value of ~ 0.7 (Fig. 4), which gradually increased and reached a value of > 0.9 in 24h, suggesting much faster chain-exchange in this case.

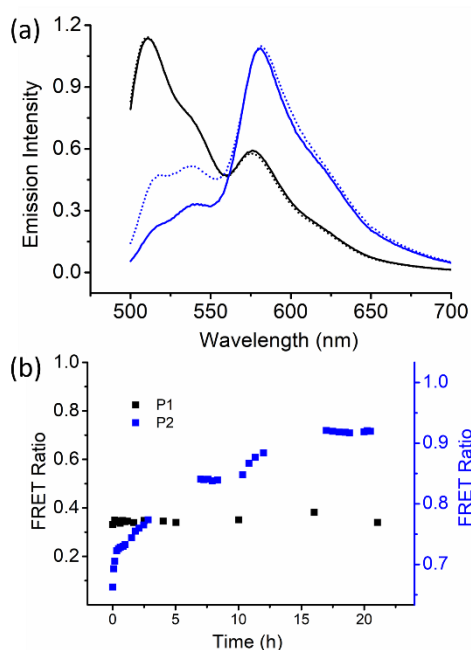
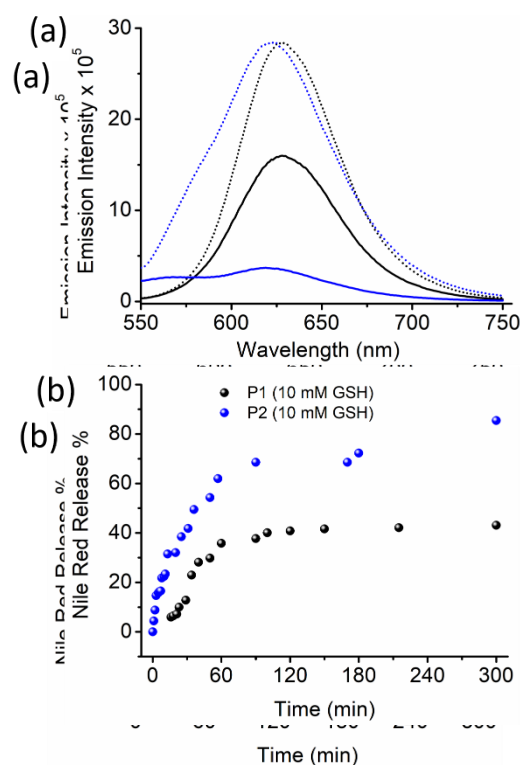


Fig. 4 (a) Emission spectra ($\lambda_{\text{ex}} = 485 \text{ nm}$) of the mixed solution of DiO and DiI encapsulated P1 (black-line) and P2 (blue line) just after mixing (dotted line) and after 24h (solid line). For P1 and P2, peak intensities were normalized to 1.0 at 520 nm and 575 nm, respectively. Concentration of polymer and each dye = $20 \mu\text{M}$ and $10 \mu\text{M}$, respectively; (b) Variation of FRET ratio as a function of time.

The contrast, as shown in Fig. 4b, is truly noteworthy as it clearly indicates that the alternating sequence leads to a much stable assembly with negligible chain exchange, which can be attributed to the crystalline nature of the assembly. Irregular sequence in P2 leads to not so effective chain-packing and consequently loosely bond aggregates and fast chain-exchange. It is noteworthy that for applications such as drug delivery and others, it is imperative to have systems with slow exchange dynamics to minimize leakage of the encapsulated therapeutic molecules. This has generally been achieved by crosslinking and other techniques.¹⁹ In that sense the present system is unique as it demonstrates crystalline assembly intrinsically can lead to a situation where the chain exchange is extremely slow.

Polydisulfides are of interest as the disulfide linkage can be cleaved in presence of glutathione (GSH), which is of biological relevance due to its significantly higher intra-cellular concentration compared to extracellular domain. GSH is a highly polar tripeptide, while the disulfide linkage in the aggregates is located in the hydrophobic domain. Hence cleavage of the disulfide bond by diffusion of the GSH to the hydrophobic pocket of the aggregates may not be very effective. Instead, earlier studies with disulfide containing small molecule surfactants predicted the cleavage may happen in the unimer state of the surfactant which always is in dynamic equilibrium with the aggregates.²⁰ In that case, sharp contrast in the chain-exchange dynamics between P1 and P2 may significantly influence the kinetics of GSH triggered disulfide cleavage and disassembly. To test such possibilities Nile red encapsulated P1 and P1 aggregates were treated with GSH (10 mM) and emission spectra of Nile red was monitored as a function of time (Fig S6, Fig. 5). To start with, Nile red emission intensity was comparable in both samples.

Fig. 5 (a) Emission spectra of Nile red encapsulated in P1 (black line) or P2 (blue line) aggregates before (dotted line) and after GSH-treatment for 5h (solid line). Concentration of Nile red, P1/ P2 and GSH = 10^{-5} M , 0.5 mg/mL , and 10 mM , respectively. $\lambda_{\text{ex}} = 530 \text{ nm}$; (b) Cumulative % release of Nile red as a function of time after GSH addition. Release % was calculated using emission intensity at 622 nm.



However, with time emission intensity decreased at much faster rate for P2 and eventually it became negligible after $\sim 5 \text{ h}$. On the other hand, for P1, the intensity reduced at much slower rate and after the same time interval still significant band intensity was noticed. % of dye release was estimated using the band intensity at 622 nm and plotted in Fig. 5b. A

clear difference can be noticed; for P2 much faster release rate was observed and after 5 h, ~ 90 % dye was released. In case of P1, much slower release rate was noted and after 5 h, only ~ 50 % dye release was noticed. Similar trend was observed when dye release experiments were performed using UV/Vis absorption spectroscopy (Fig S7). This clearly indicates a remarkable influence of the chain exchange dynamics on the rate of disassembly of these polydisulfides aggregates, which can be clearly corroborated with earlier report suggesting such disulfide cleavage happens in the unimer state of the surfactant rather in the aggregated state. It is imperative to note that depending on the specific need, both fast release and sustained release are important. Hence the ability to tune the release rate to such an extent by controlling the polymer sequence is not only of fundamental interest, but also could be of importance for practical applications.

Finally, we examined the effect of the well-ordered assembly of P1 on surface functional group display and attempted to correlate it with recognition of protein surface by electrostatic interaction. For this study, α -chymotrypsin (Cht), with cationic surface charge, was taken as the model protein.

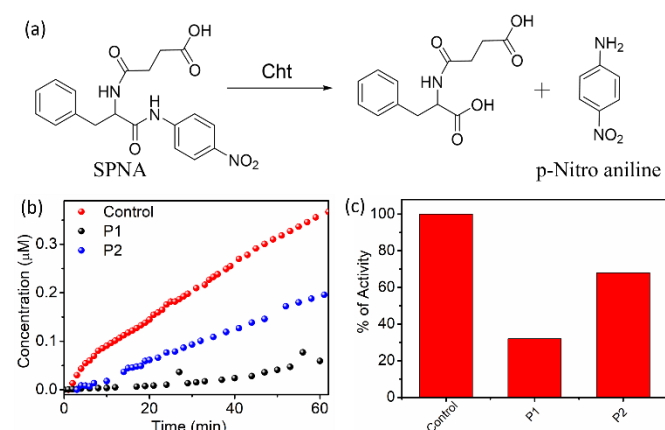


Fig. 6 (a) Scheme showing the Cht induced product formation of SPNA substrate; (b) Time versus concentration plot of para-nitroaniline generated from the hydrolysis of SPNA (2 mM) in the presence of Cht (3.2 μM) after incubation with P1 or P2 (0.1 mM) or without addition of polymer (control) at pH 9.0; (c) Relative Cht activity in presence of P1 and P2.

As the polymers are negatively charged due to the presence of the carboxylate groups, it is anticipated that they will bind to the protein surface by electrostatic interaction, which in turn will hamper the enzymatic activity of Cht, depending on the effectiveness of a given polymer aggregate to bind the protein surface.²¹ To test this, activity assays were carried out with a chromogenic substance namely N-Succinyl-L-Phenylalanine-p-nitroanilide (SPNA) (Fig. 6) It is known that Cht, in its active form, can hydrolyse SPNA, which produces p-nitro aniline having an absorption band in the visible region ($\lambda_{\text{max}} = 405 \text{ nm}$). Activity of Cht in the absence of any polymer was checked first, which showed sharp increase in the absorption intensity at 405 nm with time, indicating the protein is in its active form. Cht, preincubated with P1, showed negligible production of p-nitro aniline, indicating prominent decrease in

the enzymatic activity by ~ 70 %. On the other hand, in presence of P2, the decrease in enzymatic activity was only 30 %, significantly less than that of P1. Therefore, it is evident that the strict alternating sequence in P1, not only leads to a stable self-assembly, but also helps well-defined chain packing leading to better functional group display. This was also evident from significantly higher negative zeta potential (-32 mV) for P1 compared to -14 mV for P2. Finally, MTT assay (Fig. S8) of HeLa cell was performed with P1 and P2 (concentration up to 400 $\mu\text{g}/\text{mL}$), which showed > 85 % cells were alive even after 48 h, indicating excellent cell compatibility of the polymers and possibility of their future biomedical application.

Conclusions

In this manuscript we have demonstrated easy synthesis of an amphiphilic polydisulfide with alternating sequence of the hydrophobic and hydrophilic monomers by condensation polymerization involving thiol-activated disulfide exchange reaction. Self-assembly studies show such alternating sequence is highly useful to achieve distinct morphology and negligible chain-exchange dynamics, which can be attributed to the immiscibility driven crystalline chain-packing, that is missing in structurally similar random copolymer. Kinetic stability of the aggregate helps in slow degradation of the backbone disulfide linker in presence of glutathione, that is highly useful for sustained drug release. Furthermore, well-ordered chain packing leads to distinct ultrathin fibrillar morphology with excellent functional group (carboxylate) display, that enables electrostatic interaction mediated surface recognition of an enzyme Chymotrypsin (Cht) and ~ 70% inhibition of its enzymatic activity in contrast to the random copolymer, showing negligible enzyme-activity inhibition. Despite significant research progress in self-assembly of amphiphilic polymers and their functional utility, alternating copolymers are not so common, perhaps due to the difficulty in making such polymers with perfect alternating sequence. However, by condensation polymerization approach, one can easily have access to such polymers and results reported in this manuscript should be highly inspiring to explore such systems for diverse functional materials.

Author contributions

SB did all experimental work and collected data. Data analysis, and manuscript writing were done jointly by SB and SG. SG conceptualized the work and supervised the project and raised research funding.

Conflicts of interest

There are no conflicts to declare.

Acknowledgements

SB thanks IACS for a research fellowship. SG thanks the Technical Research Centre, IACS for funding.

Notes and references

- 1 (a) Y. Mai and A. Eisenberg, *Chem. Soc. Rev.*, 2012, **41**, 5969; (c) P. Theato, B. S. Sumerlin, R. K. O'Reilly and T. H. Epps, III, *Chem. Soc. Rev.*, 2013, **42**, 7055; (c) T. H. Epps, III and R. K. O'Reilly, *Chem. Sci.*, 2016, **7**, 1674; (d) H. Sun, C. P. Kabb, M. B. Sims and B. S. Sumerlin, *Prog. Polym. Sci.*, 2019, **89**, 61; (e) F.D. Jochum and P. Theato, *Chem. Soc. Rev.*, 2013, **42**, 7468.
- 2 (a) N. Kamaly, B. Yameen, J. Wu and O. C. Farokhzad, *Chem. Rev.*, 2016, **116**, 2602; (b) H. Cabral, K. Miyata, K. Osada and K. Kataoka, *Chem. Rev.*, 2018, **118**, 6844; (c) E. Fleige, M. A. Quadir and R. Haag, *Adv. Drug Deliv. Rev.*, 2012, **64**, 866; (d) Q. Zhang, N. R. Ko and J. K. Oh, *Chem. Commun.*, 2012, **48**, 7542; (e) R. Chacko, J. Ventura, J. Zhuang and S. Thayumanavan, *Adv. Drug Deliv. Rev.*, 2012, **64**, 836; (f) B. S. Bolu, R. Sanyal and A. Sanyal, *Molecules*, 2018, **23**, 1570; (g) S. R. Mane, A. Sathyan and R. Shunmugam, *ACS Appl. Nano. Mater.*, 2020, **3**, 2104; (h) R. Aluri, S. Saxena, D. Joshi and M. Jayakannan, *Biomacromolecules*, 2018, **19**, 2166; (i) S. Saxena and M. Jayakannan, *Biomacromolecules*, 2020, **21**, 171.
- 3 T. S. Kale, A. Klaiherd, B. Popere and S. Thayumanavan, *Langmuir*, 2009, **25**, 9660.
- 4 L. Li, K. Raghupathi, C. Song, P. Prasad and S. Thayumanavan, *Chem. Commun.*, 2014, **50**, 13417; (b) Y. Hirai, T. Terashima, M. Takenaka and M. Sawamoto, *Macromolecules*, 2016, **49**, 5084.
- 5 K. Nishimori and M. Ouchi, *Chem. Commun.*, 2020, **56**, 3473.
- 6 N. Badia and J.-F. Lutz, *Chem. Soc. Rev.*, 2009, **38**, 3383.
- 7 (a) S. G. Fenimore, L. Abezgauz, D. Danino, C. C. Ho and C. C. Co, *Macromolecules*, 2009, **42**, 2702; (b) M. Ueda, A. Hashidzume and T. Sato, *Macromolecules*, 2011, **44**, 2970; (c) K. Nishimori, E. Cazares-Cortes, J. M. Guigner, F. Tournilhac and M. Ouchi, *Polym. Chem.*, 2019, **10**, 2327; (d) B. Saha, N. Choudhury, S. Seal, B. Ruidas and P. De, *Biomacromolecules*, 2019, **20**, 546.
- 8 (a) E. Zhao, J. W. Y. Lam, L. M. Meng, Y. Hong, H. Q. Deng, G. X. Bai, X. H. Huang, J. H. Hao and B. Z. Tang, *Macromolecules*, 2015, **48**, 64. (b) B. Saha, K. Bauri, A. Bag, P. K. Ghorai and P. De, *Polym. Chem.*, 2016, **7**, 6895. (c) J. J. Yan, Z. K. Wang, X. S. Lin, C. Y. Hong, H. J. Liang, C. Y. Pan and Y. Z. You, *Adv. Mater.*, 2012, **24**, 5617. (d) B. Saha, N. Choudhury, A. Bhadrani, K. Bauri and P. De, *Polym. Chem.*, 2019, **10**, 3306.
- 9 T. Wagner-Jauregg, *Ber. Dtsch. Chem. Ges. B*, 1930, **63**, 3213.
- 10 R. Barman, A. Mukherjee, A. Nag, P. Rajdev and S. Ghosh, *Chem. Commun.*, 2023, **59**, 13951.
- 11 V. Damodara, H. Sardana, and S. Ramakrishnan, *Eur. Polym. J.*, 2024, 112818.
- 12 D. Basak, R. Kumar and S. Ghosh, *Macromol. Rapid Commun.*, 2014, **35**, 1340.
- 13 (a) R. Bej, P. Dey and S. Ghosh, *Soft Matter.*, 2020, **16**, 11; (b) I. Altinbasak, M. Arslan, R. Sanyal and A. Sanyal, *Polym. Chem.*, 2020, **11**, 7603; (c) J. Zhuang, M. Gordon, J. Ventura, L. Li and S. Thayumanavan, *Chem. Soc. Rev.*, 2013, **42**, 7421; (c) J. Quinn, M. Whittaker and T. Davis, *Polym. Chem.*, 2017, **8**, 97; (d) H. Mutlu, E. B. Ceper, X. Li, J. Yang, W. Dong, M. M. Ozmen and P. Theato, *Macromol. Rapid Commun.*, 2019, **40**, 1800650; (e) J.-H. Ryu, S. Jiwpanich, R. Chacko, S. Bickerton and S. Thayumanavan, *J. Am. Chem. Soc.*, 2010, **132**, 8246; (f) I. Altinbasak, S. Kocak, R. Sanyal, and A. Sanyal, *Biomacromolecules*, 2022, **23**, 3525.
- 14 (a) G. K. Such, Y. Yan, A. P. R. Johnston, S. T. Gunawan and F. Carus, *Adv. Mater.*, 2015, **27**, 2278; (b) A. Russo, W. DeGraff, N. Friedman and J. B. Mitchell, *Cancer Res.*, 1986, **46**, 2845; (c) F. Q. Schafer and G. R. Buettner, *Free Radic. Biol. Med.*, 2001, **30**, 1191.
- 15 (a) J. C. Foster, S. Varlas, B. Couturaud, Z. Coe and R. K. O'Reilly, *J. Am. Chem. Soc.*, 2019, **141**, 2742; (b) A. Sikder, S. Chakraborty, P. Rajdev, P. Dey and S. Ghosh, *Acc. Chem. Res.*, 2021, **54**, 2670. View Article Online
DOI: 10.1039/D4NR02494J
- 16 (a) X. He, Y. He, M.-S. Hsiao, R. L. Harniman, S. Pearce, M. A. Winnik, I. Manners, *J. Am. Chem. Soc.*, 2017, **139**, 9221; (b) X. He, M. S. Hsiao, C. E. Boott, R. L. Harniman, A. Nazemi, X. Li, M. A. Winnik, I. Manners, *Nat. Mater.*, 2017, **16**, 481; (c) M. Inam, G. Cambridge, A. Pitto-Barry, Z. P. L. Laker, N. R. Wilson, R. T. Mathers, A. P. Dove, R. K. O'Reilly, *Chem. Sci.*, 2017, **8**, 4223; (d) P. J. Hurst, A. M. J. Rakowski, P. Patterson, *Nat. Commun.*, 2020, **11**, 4690; (e) A. Rajak and A. Das, *Angew. Chem. Int. Ed.*, 2022, **61**, e202116572.
- 17 C. Zhang, H. Pan and Y. Zhou, *Macromolecules*, 2023, **56**, 7870.
- 18 P. Rajdev and S. Ghosh, *J. Phys. Chem. B*, 2019, **123**, 327.
- 19 (a) J.-H. Ryu, R. T. Chacko, S. Jiwpanich, S. Bickerton, R. P. Babu and S. Thayumanavan, *J. Am. Chem. Soc.*, 2010, **132**, 17227; (b) P. Rajdev, D. Basak, and S. Ghosh, *Macromolecules*, 2015, **48**, 3360.
- 20 S. Ghosh, K. Irvine and S. Thayumanavan, *Langmuir*, 2007, **23**, 7916.
- 21 (a) H. S. Park, Q. Lin and A. D. Hamilton, *J. Am. Chem. Soc.*, 1999, **121**, 8; (b) B. S. Sandanaraj, D. R. Vutukuri, J. M. Simard, A. Klaiherd, R. Hong, V. M. Rotello and S. Thayumanavan, *J. Am. Chem. Soc.*, 2005, **127**, 10693; (c) M. De, S. S. Chou, V. P. Dravid, *J. Am. Chem. Soc.*, 2011, **133**, 17524; (d) A. Sikder, A. Das and S. Ghosh, *Angew. Chem. Int. Ed.*, 2015, **54**, 6755; (e) P. Khanra, P. Rajdev and A. Das, *Angew. Chem. Int. Ed.*, 2024, **63**, e202400486.

Journal Name

ARTICLE

View Article Online
DOI: 10.1039/D4NR02494J

Published on 26 agosto 2024. Downloaded on 8/9/2024 05:21:41.

Nanoscale Accepted Manuscript

The data supporting this article have been included as part of the Supplementary Information [View Article Online](#)
DOI: 10.1039/D4NR02494J

Nanoscale Accepted Manuscript